Geophysical Research Letters

RESEARCH LETTER
10.1029/2018GL077852

**Key Points:**
- Lapse rate feedback is the largest contributor to Arctic amplification relative to the tropics
- Lapse rate feedback is consistently comparable to surface albedo feedback over the Arctic
- Estimated net cloud feedback over the Arctic is largely uncertain including its sign

**Supporting Information:**
- Supporting Information S1

**Correspondence to:**
R. Zhang and H. Wang,
rdzhangeos@gmail.com;
hailong.wang@pnnl.gov

**Citation:**
Zhang, R., Wang, H., Fu, Q., Pendergrass, A. G., Wang, M., Yang, Y., et al. (2018). Local radiative feedbacks over the Arctic based on observed short-term climate variations. *Geophysical Research Letters*, *45*, 5761–5770. https://doi.org/10.1029/2018GL077852

Received 8 MAR 2018
Accepted 23 MAY 2018
Accepted article online 30 MAY 2018
Published online 12 JUN 2018



# Local Radiative Feedbacks Over the Arctic Based on Observed Short-Term Climate Variations

**Rudong Zhang[1,2,3], Hailong Wang[3], Qiang Fu[4], Angeline G. Pendergrass[5], Minghuai Wang[1,2], Yang Yang[3], Po-Lun Ma[3], and Philip J. Rasch[3]**

[1]Institute for Climate and Global Change Research and School of Atmospheric Sciences, Nanjing University, Nanjing, China, [2]Jiangsu Provincial Collaborative Innovation Center of Climate Change, Nanjing, China, [3]Atmospheric Sciences and Global Change Division, Pacific Northwest National Laboratory, Richland, WA, USA, [4]Department of Atmospheric Sciences, University of Washington, Seattle, WA, USA, [5]National Center for Atmospheric Research, Boulder, CO, USA

**Abstract** We compare various radiative feedbacks over the Arctic (60–90°N) estimated from short-term climate variations occurring in reanalysis, satellite, and global climate model data sets using the combined Kernel-Gregory approach. The lapse rate and surface albedo feedbacks are positive, and their magnitudes are comparable. Relative to the tropics (30°S–30°N), the lapse rate feedback is the largest contributor to Arctic amplification among all feedbacks, followed by surface albedo feedback and Planck feedback deviation from its global mean. Both shortwave and longwave water vapor feedbacks are positive, leading to a significant positive net water vapor feedback over the Arctic. The net cloud feedback has large uncertainties including its sign, which strongly depends on the data used for all-sky and clear-sky radiative fluxes at the top of the atmosphere, the time periods considered, and the methods used to estimate the cloud feedback.

**Plain Language Summary** The Arctic has warmed dramatically in recent decades, with temperature increasing at a rate of about twice as fast as the global mean value. This phenomenon, commonly known as Arctic amplification, has been found in the observed and modeled climate changes. Several feedback mechanisms have been shown to contribute to Arctic amplification, but their relative importance is still very uncertain. Here we use a variety of reanalysis and satellite data sets to quantify the Arctic local feedbacks based on short-term climate variations, evaluate the feedbacks simulated in a global climate model, diagnose the impact of data set choices on the feedback estimates, and identify the sources of main uncertainties. The most disagreement is found in the estimate of cloud feedback.

## 1. Introduction

The concept of climate feedback offers a powerful framework to characterize the response of the climate system to an external radiative forcing (Charney et al., 1979; Hansen et al., 1984). The response to a positive net radiative imbalance ($\Delta R$) at the top of the atmosphere (TOA) caused by radiative forcing ($\Delta Q$) leads to a surface warming ($\Delta T_s$) as described by the formula $\Delta R = \Delta Q + \lambda \Delta T_s$, where $\lambda$ is the net climate feedback parameter (e.g., Bony et al., 2006). Feedbacks are usually given as the first-order terms in a Taylor series expansion through the equation $\lambda = \partial R/\partial T_s = \sum \frac{\partial R}{\partial x}\frac{\partial x}{\partial T_s} = \sum \lambda_x$, where $x$ denotes temperature, water vapor (WV), surface albedo, or clouds (e.g., Shell et al., 2008). The temperature feedback can be further separated into the Planck feedback (due to vertically uniform temperature change) and the lapse rate (LR) feedback (due to departures from surface temperature change at each vertical level). Climate feedbacks play an important role in determining the climate sensitivity, defined as the equilibrium temperature change in response to the radiative forcing from a doubling of atmospheric $CO_2$ concentration, which has a large spread among global climate models (Intergovernmental Panel on Climate Change (IPCC), 2013).

The Arctic has warmed more than twice the global mean since the mid-1950s and, in particular, more than six times the global mean since the late 1990s (Huang et al., 2017). This is a phenomenon commonly known as Arctic amplification (AA), which has been found in the observed and modeled climate changes (IPCC, 2013). Several feedbacks such as albedo feedback (Manabe & Wetherald, 1975), temperature feedback (Pithan & Mauritsen, 2014), and cloud feedback (Vavrus, 2004) have been reported to contribute to AA. The surface longwave emissivity and associated feedbacks are also found to have discernable impact on the outgoing longwave radiation and surface temperature in the Arctic (Feldman et al., 2014; Huang et al., 2018). There are, however, uncertainties and disagreement about the role of different feedbacks. The albedo feedback

has often been considered as the main contributor (e.g., Screen & Simmonds, 2010; Taylor et al., 2013). However, Winton (2006) reported that it is not a dominating factor in the simulated AA, and AA still exists in a coupled climate model with locked albedo (Graversen & Wang, 2009). Pithan and Mauritsen (2014) found that AA is dominated by temperature feedback, while albedo feedback plays a less important role based on preindustrial control and $4\times CO_2$ experiments from the CMIP5 (Coupled Model Intercomparison Project phase 5; Taylor et al., 2012). Ideally, the magnitude of feedbacks would be estimated from long-term observations covering decades or even centuries, but there are no such long-term observational records, especially for atmospheric WV, temperature, and clouds. However, the relatively short observational data can still be used to constrain modeled feedback estimates (e.g., Dessler, 2010, 2013). But systematic estimate of feedbacks based on observed short-term climate variations over the Arctic has received relatively little attention, particularly from a local perspective (Po-Chedley et al., 2018; Roe et al., 2015).

Here we use reanalysis products, satellite data, and global climate model experiments to (i) estimate the magnitude of radiative feedbacks over the Arctic (60–90°N) based on short-term climate variations, (ii) evaluate the modeled feedbacks with respect to observations at the TOA, and (iii) diagnose the impact of data set choices on the feedback estimates.

## 2. Methodology

### 2.1. Model and Data

The Community Atmosphere Model version 5 (CAM5; Neale et al., 2010) is configured in nudging mode (Ma et al., 2013), where the model wind fields are nudged to agree with MERRA (Modern Era Retrospective-Analysis for Research and Applications) reanalysis products (Rienecker et al., 2011). While other meteorological fields are allowed to evolve freely according to model physics, the wind nudging is applied to CAM5 to ensure that the large-scale circulation patterns can be accurately captured. The latter is important for the transport of heat, moisture, and aerosols to the Arctic (e.g., Ma et al., 2013). Sea surface temperatures and sea ice concentrations are prescribed with time-varying observations. The model is run with a horizontal grid spacing of $1.9 \times 2.5°$ and 30 vertical layers. The simulation covers the period from 1979 to 2014. Monthly mean anthropogenic and open biomass burning emissions (available up to 2014) from the recently released data sets for phase 6 of CMIP are used here (Yang et al., 2017). A set of model improvements in the representation of aerosol-cloud microphysical processes and a four-mode version of the Modal Aerosol Module are included to better characterize the vertical distribution of aerosols and their transport to the Arctic (Liu et al., 2016; Wang et al., 2013, 2014).

The ERA-Interim reanalysis provided by ECMWF (European Centre for Medium-Range Weather Forecasts) (Dee et al., 2011), the Japanese 55-year reanalysis (JRA-55) provided by the Japan Meteorological Agency (Kobayashi et al., 2015), and the MERRA and MERRA-2 (version 2; Bosilovich & Koster, 2015) reanalysis provided by National Aeronautics and Space Administration (NASA) are used in this study. The NASA Clouds and the Earth's Radiant Energy System (CERES) Energy Balanced and Filled (EBAF) products are also used (CERES Science Team, 2017). The latest EBAF-TOA Ed4.0 (version 4.0) products cover the period from March 2000 to September 2017, which have many improvements with respect to the previous version (version 2.8, Loeb et al., 2009) including the use of advanced and more consistent input data, instrument calibration, and retrieval of cloud properties (Loeb et al., 2018).

### 2.2. The Local Radiative Feedback Framework

The net radiative energy budget at the TOA, $R$, is positive when the Earth-atmosphere system gains energy. For global mean, we always have $R = 0$ if the system is at equilibrium. When the system moves away from the equilibrium in response to a radiative forcing $\Delta Q$, the change in $R$ can be related to $\Delta Q$ and surface temperature change $\Delta T_s$ in a form

$$\Delta R = \Delta Q + \lambda \Delta T_s,$$

where $\lambda$ is the net climate feedback parameter. When the system reaches a new equilibrium, $\Delta R$ becomes 0, and thus

$$\Delta T_s = -\Delta Q/\lambda.$$

In considering any regional system (e.g., the Arctic), we define $H$ as the horizontal heat flux convergence to the system. At equilibrium we always have $R + H = 0$. When the system moves away from the equilibrium in response to a radiative forcing $\Delta Q$, we also have

$$\Delta R = \Delta Q + \lambda \Delta T_s.$$

When the regional system reaches a new local equilibrium, $\Delta R + \Delta H = 0$, where $\Delta H$ is the change in $H$, and thus, $\Delta R = -\Delta H$. We therefore have

$$\Delta T_s = -(\Delta Q + \Delta H)/\lambda.$$

The $\lambda$ above can be separated into Planck feedback ($\lambda_0$) and feedbacks ($\lambda_x$) due to changes in the LR, surface albedo, WV, and clouds so that $\lambda = \lambda_0 + \sum \lambda_x$ (e.g., Cai & Lu, 2007; Crook et al., 2011; Feldl et al., 2017; Goosse et al., 2018; Pithan & Mauritsen, 2014; Rose et al., 2014). The $\lambda$ must be negative for a stable climate system.

### 2.3. Combined Kernel-Gregory Method

Climate variables used in the feedback calculation include absorbed shortwave (SW), longwave radiation (LW), net radiation (NET = SW + LW) at the TOA, surface albedo ($\alpha$), temperature profile ($T$), WV profile ($q$), and surface air temperature (SAT). Albedo $\alpha$ is calculated as the ratio of upward to downward shortwave fluxes at the surface. Monthly anomalies (denoted by $\Delta$) of each climate variable are calculated from the corresponding monthly time series by subtracting its respective monthly mean climatology for each grid, level (for variables including a vertical dimension), and month. In the calculation of WV feedback, the moisture change is associated with both vertically uniform warming and the deviations from vertically uniform warming with fixed relative humidity.

Total SW, LW, and NET feedbacks are calculated using the regression-based Gregory method (Gregory et al., 2004) from a local perspective (Feldl & Roe, 2013). The area average of $\Delta$SW, $\Delta$LW, $\Delta$NET, and $\Delta$SAT over the Arctic is computed first, and then a 12-month running mean is applied to the time series of these anomalies, following Hwang et al. (2017), to retain radiative feedback processes with timescales spanning longer than a month. After that, the TOA flux anomalies are regressed onto the SAT anomalies to obtain the linear regression coefficient. According to the definition $\Delta R = \Delta Q + \lambda \Delta T_s$, we need to further deduct the $\Delta Q/\Delta T_s$ based on this regression coefficient to obtain the total feedbacks, where the $\Delta Q/\Delta T_s$ is calculated from relevant data in Pendergrass et al. (2018) and shown in the Table S1.

Individual feedback components of $\alpha$, $T$, and $q$ are calculated using the combined Kernel-Gregory method (Soden & Held, 2006) in the following steps.

Step 1 Anomalies ($\Delta x$, where $x$ is $\alpha$, $T$, or $q$) are multiplied by the respective radiative kernel ($K_x = \partial R/\partial x$) at each grid, level (for $T$ and $q$) and month to produce the associated all-sky TOA radiative flux anomalies ($\Delta R_x = K_x \Delta x$) with the spatial distribution preserved. The $\Delta T$ is set to $\Delta$SAT at each vertical level for the Planck feedback calculation, and $\Delta T$ is the anomalous departure of temperature at each level from SAT in the calculation of LR feedback.

Step 2 $\Delta R_x$ of $T$ and $q$ at each vertical level are summed to produce the cumulative radiative response at the TOA (Dalton & Shell, 2013). For the Planck feedback calculation, this integration includes the surface as well.

Step 3 The area-average $\Delta R_x$ of $\alpha$, $T$, and $q$ is calculated over the Arctic and then a 12-month running mean is applied.

Step 4 The TOA flux anomalies are regressed onto the SAT anomalies to obtain feedbacks (i.e., the slope of the linear least squares fit).

Cloud feedback is calculated with two different methods. One is called the residual method (Soden & Held, 2006), in which the feedback is calculated as follows. First, $\Delta R_x$ of $\alpha$, $T$, and $q$ is subtracted from the TOA all-sky flux anomalies ($\Delta R_{\mathrm{all-sky}}$) to produce cloud forcing anomalies ($\Delta R_{\mathrm{cloud}} = \Delta R_{\mathrm{all-sky}} - \sum \Delta R_x$) at each grid and month. Next, the area average of $\Delta R_{\mathrm{cloud}}$ over the Arctic is calculated and then a 12-month running mean is applied. Finally, the monthly cloud forcing anomalies are regressed onto the SAT anomalies to obtain the linear regression coefficient. As in the total feedback calculation, we also need to further deduct the $\Delta Q/\Delta T_s$ based on this regression coefficient to obtain the cloud feedback (residual).

The other method for cloud feedback calculation is referred to as the adjustment method (Soden et al., 2008). First, the cloud radiative forcing (CRF) anomalies are calculated as the change in difference between the all-sky and the clear-sky TOA flux, i.e., $\Delta\mathrm{CRF} = \Delta(R_{\mathrm{all-sky}} - R_{\mathrm{clear-sky}})$, at each grid and month. The ΔCRF is then adjusted to account for environmental masking from $\Delta R_x$ of $\alpha$, $T$, and $q$, yielding $\Delta R_{\mathrm{cloud}} = \Delta\mathrm{CRF} + \sum\left(\Delta R_x^0 - \Delta R_x\right)$, where $\Delta R_x^0$ represents the clear-sky $\Delta R_x$ (using the clear-sky kernels). Following similar steps in the residual method, the area average of $\Delta R_{\mathrm{cloud}}$ over the Arctic and monthly anomalies are calculated to obtain the linear regression coefficient. Finally, we need to further add the radiative forcing difference under clear-sky ($\Delta Q^0$) and all-sky ($\Delta Q$) conditions scaled by the surface temperature change (i.e., $\Delta(Q^0 - Q)/\Delta T_s$) to obtain the cloud feedback (adjustment). Here the $\Delta(Q^0 - Q)/\Delta T_s$ due to greenhouse gases and aerosols is calculated from relevant data in Pendergrass et al. (2018) and shown in Table S2.

In the calculations above we have to use a substitute for the effect of radiative forcing due to a lack of associated temporal information in the available data sets, which is a common issue for calculating short-term feedbacks (Koumoutsaris, 2013). Here the monthly radiative kernels are derived from the large-ensemble simulations of CAM5 (Pendergrass et al., 2018). Note that positive TOA fluxes are defined as downwelling. Thus, positive feedback values mean energy gain in the climate system. Hereafter, unless otherwise specified, the uncertainty of feedback estimates is provided as the 95% confidence interval of the linear regression fit.

## 3. Results

### 3.1. Arctic Feedbacks Estimated From 35-Year (1980–2014) CAM5 and Reanalysis

The Arctic local feedbacks are calculated for SW, LW, and NET radiative fluxes. The red dots in Figure 1 show the estimates of feedbacks based on 35-year (1980–2014) CAM5, ERA-Interim, JRA-55, and MERRA data sets. Table S3 in the supporting information presents the values of red dots in Figure 1. As the most straightforward climate feedback, the Planck feedback is essentially indistinguishable among the four data sets, with very small uncertainty. The coefficient of determination ($R^2$) nearly equals 1 (see Table S3). While the WV feedback is weak in all four data sets, it is positive over the Arctic, and its magnitude is comparable between the SW and LW. Among the NET feedbacks, the albedo and LR feedbacks are comparable. Net cloud feedback is negative in the three reanalysis data sets when calculated with both the adjustment and residual methods (described in section 2.3). In contrast, the net cloud feedback is close to zero in CAM5, mainly resulting from the difference of SW cloud feedback between CAM5 and reanalysis results. The $R^2$ for LR, albedo, and WV feedbacks are larger than 0.5. However, the correlation between $\Delta R_{\mathrm{cloud}}$ and ΔSAT is weak, especially for CAM5 ($R^2$ is almost zero), indicating that factors other than SAT are more important in regulating $\Delta R_{\mathrm{cloud}}$. Like the cloud feedback, the total feedback also has large spread among the four data sets. The total net feedback is negative in all three reanalysis data sets, which is expected for a system at equilibrium ($\Delta R + \Delta H = 0$; see section 2.2). However, like the net cloud feedback, the total net feedback in CAM5 is also close to zero due to the larger SW total feedback relative to the reanalysis results.

### 3.2. Arctic Feedbacks Based on CAM5 and Reanalysis Combined With CERES Measurements

There has been considerable debate about net cloud feedback in the Arctic. Using the CMIP5 multimodel framework but different methods, Zelinka et al. (2013) reported a negative cloud feedback in the Arctic, while Pithan and Mauritsen (2014) showed a slightly positive ensemble mean with disagreement on the sign among individual models. Using surface observations, Eastman and Warren (2010a, 2010b) showed that cloud changes appear to enhance the Arctic warming. Meteorological fields ($\alpha$, $T$, and $q$) from reanalysis combined with satellite radiative flux measurements at the TOA provide an effective way to estimate the cloud feedback (Dessler, 2010, 2013). Here we examine how the CERES products combined with CAM5 and reanalysis data sets impact the estimate of Arctic feedbacks. We first repeat the feedback calculations for the period (March 2000 to December 2014) when model/reanalysis overlaps with CERES products to facilitate the comparison later. Results from the 15-year analysis are marked with blue dots in Figure 1 and the values in Table S4. Comparing to the 35-year results, except for the Planck feedback, estimates of other feedbacks have discernable differences along with an increase in uncertainty in all four data sets, especially in CAM5. In particular, the total and cloud feedbacks have large differences between the 35-year and 15-year calculations. The increased uncertainty in cloud feedback is mostly associated with its SW component (e.g., Vial et al., 2013). Interestingly, the net total and cloud feedbacks derived from the 15-year CAM5 simulation become

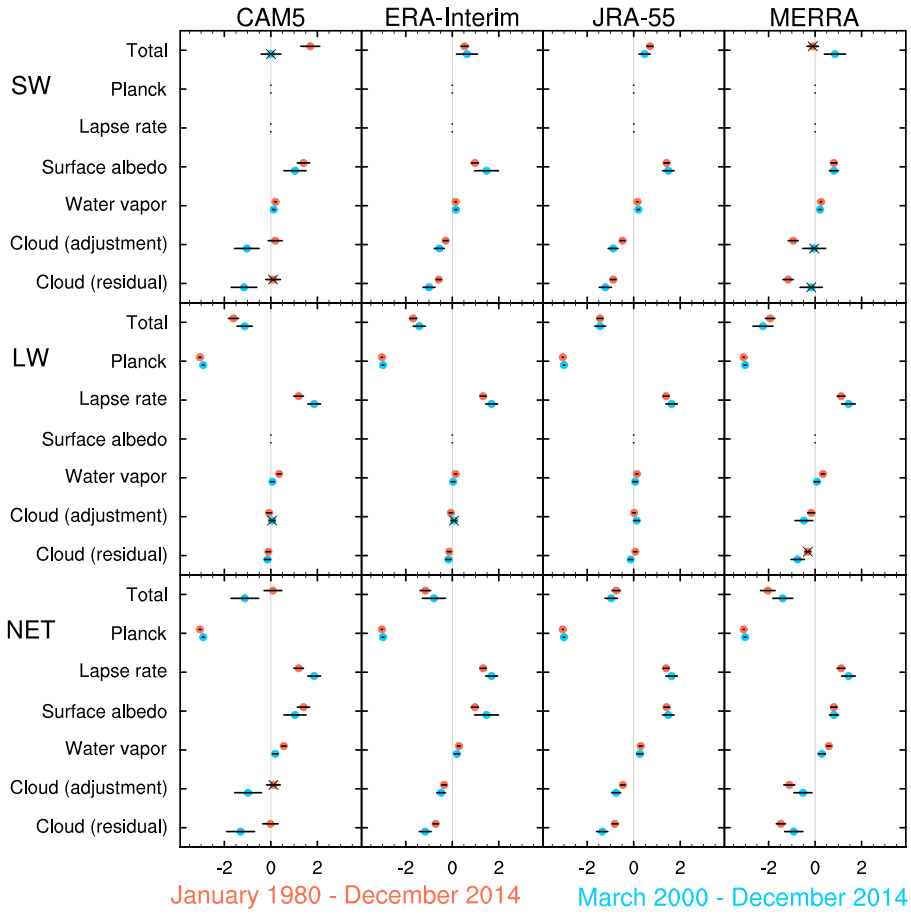


**Figure 1.** Local individual radiative feedbacks ($W \cdot m^{-2} \cdot K^{-1}$) at the TOA over the Arctic. The black error bar represents the uncertainty of each feedback. The black cross symbol indicates an insignificance at the 95% confidence level. The red dots and blue dots use data sets during January 1980 to December 2014 and March 2000 to December 2014, respectively.

consistent in sign with the reanalysis results due to the dramatic change in the SW component. Meanwhile, the SW total feedback in MERRA results also changed dramatically. The sensitivity of cloud (and total) feedbacks to the length of data sets being used in the analysis reflects the impact of internal climate variability on the feedback estimation using short-term data sets (Armour et al., 2013; Dalton & Shell, 2013). Next, we will discuss how the inclusion of satellite measurements in the data sets affects the feedback estimation.

We repeat the 15-year feedback calculations to incorporate satellite measurements, that is, using the radiative fluxes at the TOA from CERES to replace the corresponding fluxes in CAM5 or reanalysis. Results are compared in Figure 2, where blue dots are replotted from Figure 1 to facilitate the comparison and red dots denote the feedbacks from CAM5 or reanalysis combined with CERES for both all-sky and clear-sky TOA radiative fluxes. The green dots represent similar calculations to the red dots but only with CERES all-sky fluxes incorporated. The numerical values for red and green dots in Figure 2 are documented in Tables S5 and S6, respectively. According to the methodology described in section 2.3, the LR, albedo, and WV feedbacks are independent of the radiative flux changes at the TOA. Therefore, only the total and cloud feedback differs from each other over the same period.

The difference of CERES-based total feedback (red or green dots) among the four data sets indicates that the total feedback calculation is sensitive to the SAT choices because they use the same all-sky CERES fluxes. While the CERES-based total feedbacks have the same signs with the blue-dot cases in the SW and LW components, respectively, the signs of net total feedbacks become positive after using CERES fluxes as a result of larger positive SW total feedbacks. We will further discuss this issue in section 3.3. The residual method for

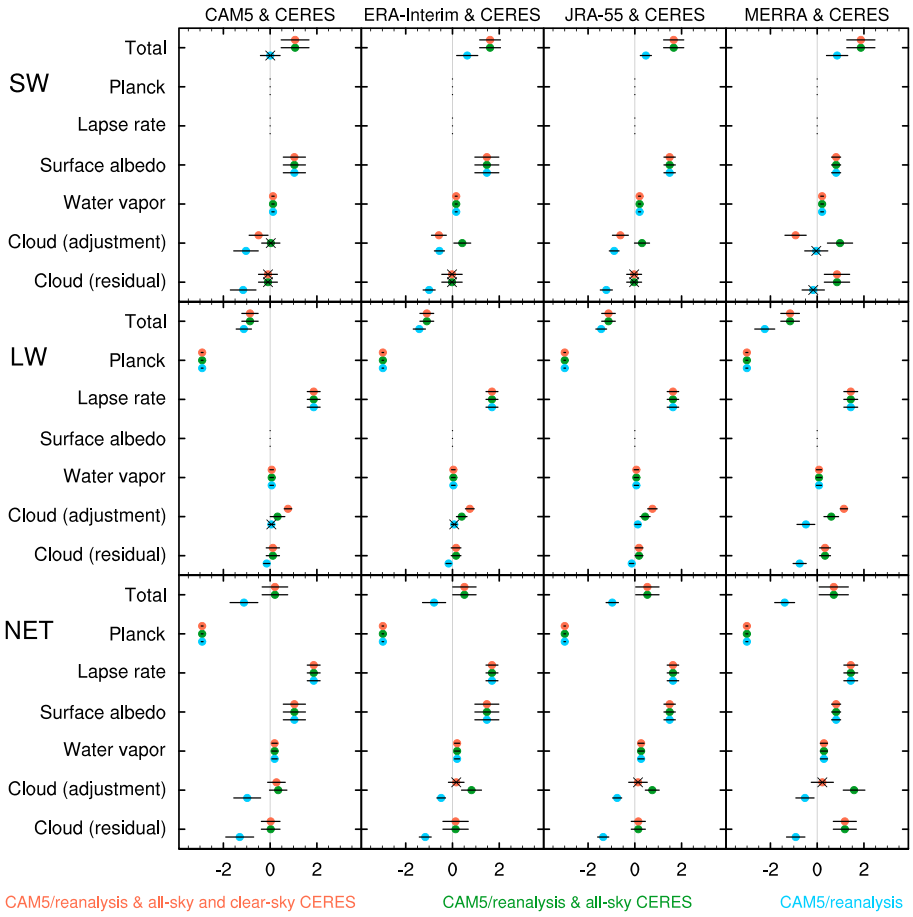


**Figure 2.** Same as Figure 1 but both all-sky and clear-sky radiative fluxes at the TOA (red dots) and all-sky radiative fluxes at the TOA (green dots) use CERES EBAF-TOA Ed4.0 products instead of model/reanalysis results. The blue dots are replotted from Figure 1 for comparison. Data sets used in the calculations are for the period of March 2000 to December 2014.

cloud feedback calculation described in section 2.3 does not require clear-sky TOA fluxes ($R_{\mathrm{clear-sky}}$), so the cloud feedbacks (residual) are identical between red dots and green dots in Figure 2. Owing to smaller LR and albedo feedbacks, the net cloud feedback (residual) has a markedly positive value in MERRA and CERES results relative to other data sets. This is a weakness of the residual method because the cloud feedback is not computed directly (Soden & Held, 2006), so the adjustment method is recommended (Soden et al., 2008).

To further diagnose the impact of $R_{\mathrm{clear-sky}}$ on the cloud feedback calculation, we can compare the cloud feedback derived from the adjustment method between red dots and green dots in Figure 2. Using $R_{\mathrm{clear-sky}}$ from CAM5 or reanalysis can produce a wide spread in cloud feedbacks among the four data sets (green dots). Compared to the green-dot cases, the dramatic change is the sign of SW cloud feedback, from positive to negative, when both $R_{\mathrm{all-sky}}$ and $R_{\mathrm{clear-sky}}$ from CERES are included in the calculation (red dots). It is no surprise that cloud feedbacks tend to be consistent and have a smaller spread among the four data sets when more satellite measurements are included in the calculation. However, the net cloud feedbacks (red dots) are still not significant at the 95% confidence level.

### 3.3. Comparison of Feedbacks Between the Arctic and Tropics

To maximize the use of latest data sets and expand our vision to the global scale, we calculate feedbacks from the zonal-mean perspective using 18-year (March 2000 to September 2017) data sets for three cases: reanalysis (ERA-Interim, JRA-55, and MERRA-2), reanalysis combined with all-sky CERES (using all-sky CERES fluxes to replace the corresponding fluxes in the reanalysis), and reanalysis combined with all-sky and clear-sky CERES (using both all-sky and clear-sky CERES fluxes to replace the corresponding fluxes in the reanalysis).

Figures S2a–S2i show zonal-mean feedbacks calculated via the regression onto zonal-mean SAT anomalies. The meridional distribution of Planck feedback is nearly the same in all three data sets. The LR feedback is positive at extratropical latitudes where the LR is constrained by baroclinic adjustment, but negative where the temperature profile is close to a moist adiabat (Bony et al., 2006). As expected from the distribution of snow and ice, the albedo feedback is focused on the high latitudes (Hall, 2004). The WV feedback is positive over all latitudes, stronger in the tropics where moisture changes are stronger (Held & Soden, 2000), and dominated by its LW component. Owing to complex interactions among clouds of different thicknesses, heights, and optical properties (e.g., Bony et al., 2015; Zelinka & Hartmann, 2012; Zhou et al., 2013), cloud feedback (calculated using the adjustment method) is more complex than other feedbacks and has larger spread among the three data sets (Figure S2g) mainly from its SW component (Figure S3a). The meridional distribution pattern of cloud feedback is opposite between its SW and LW component (Figure S3), indicating a large disagreement of cloud fields between the different reanalysis data sets. The cloud feedback is more consistent among the three data sets when more CERES products are used in the calculation (Figures S2h and S2i). This indicates that the choice of data sets for meteorological fields ($\alpha$, $T$, and $q$) has a small impact on the inferred cloud feedback, which mainly depends on the CRF (i.e., CRF = $R_{\mathrm{all\ -\ sky}} - R_{\mathrm{clear\ -\ sky}}$). Figure S4 further diagnoses the impact of $R_{\mathrm{clear\ -\ sky}}$ on the cloud feedback estimates. $R_{\mathrm{clear\ -\ sky}}$ from CERES does have significant influences on the inferred cloud feedback, especially its SW component (Figure S4a). This significant difference might be due to CERES $R_{\mathrm{clear\ -\ sky}}$ only sampling the sky without clouds (Loeb et al., 2018). In Figure 2, the CERES-based net total feedback is positive. We replot Figure 2 but using the 18-year data sets (see Figure S5), where the net total feedback is close to zero, even with a negative value in MERRA-2 results ($-0.03\ \mathrm{W \cdot m^{-2} \cdot K^{-1}}$). Zonal mean net total feedback calculated with the CERES fluxes does increase at almost all latitudes (see Figure S7) due to the increase in its SW component, but almost all net total feedbacks are negative. The comparison between Figures 2 and S5 once again reflects the impact of internal climate variability on the feedback estimation. Another possible reason for positive net total feedback is related to the term $\Delta Q/\Delta T_s$ (Figure S6) that was derived from a different data set (see section 2.3).

As shown in Figure S2a, Planck feedback is the most fundamental quantity. From a local perspective on feedback definition, we can treat the global mean Planck feedback as the reference response, and then calculate the local deviation of Planck feedback from its global mean. Based on the zonal-mean feedbacks, we further make a scatter plot for regional feedbacks between the Arctic and the tropics (30°S–30°N) to explore the main contributor to AA relative to the tropics (see Figure 3a). The values for variables in Figure 3a are in Tables S7–S9. Except for the uncertain cloud feedback, all feedbacks (including the Planck feedback deviation) are positive over the Arctic. The Planck feedback deviation, albedo, and LR feedbacks all contribute to AA, relative to the tropics (above the 1:1 line in Figure 3a). The magnitudes of LR and albedo feedbacks are comparable, but the LR feedback is the largest contributor to AA among these feedbacks, followed by the albedo feedback and Planck feedback deviation according to their distance to the 1:1 line. This ranking is the same as the results derived from the CESM large-ensemble simulations (purple symbols in Figure 3a) in Pendergrass et al. (2018) and the CMIP5 multimodel ensemble mean in Pithan and Mauritsen (2014). The sign of LW cloud feedback over the Arctic is positive and consistent among three cases (Figure S3g), but the sign for SW cloud feedback is uncertain. As a result, the sign of net cloud feedback over the Arctic in Figure 3a is uncertain and strongly depends on the data used for all-sky and clear-sky radiative fluxes at the TOA. Compared to the Arctic, the sign of cloud feedback over the tropics is more uncertain, even for its LW component (Figure S3g).

## 4. Discussion and Summary

Although we focus on the feedbacks over the Arctic in this study, a closely relevant topic is the change in global and annual mean SAT when accounting for the various feedbacks affecting the global climate, that is, the climate sensitivity (IPCC, 2013). Meanwhile, it is also interesting to further evaluate our analysis on a global scale. For these purposes, we compare global-mean feedbacks calculated from the short-term data sets with other results derived from long-term coupled simulations (Block & Mauritsen, 2013; Pendergrass et al., 2018; Soden et al., 2008; Vial et al., 2013) in Figure 3b. The short-term results are comparable to the long-term ones except for the cloud feedback. The global mean cloud feedback is negative in two of the three cases using reanalysis only (see Figure S8), resulting in a mean value close to zero. When incorporating the CERES fluxes, global mean cloud feedbacks become positive and consistent with other studies. As shown in Figures 1, 2

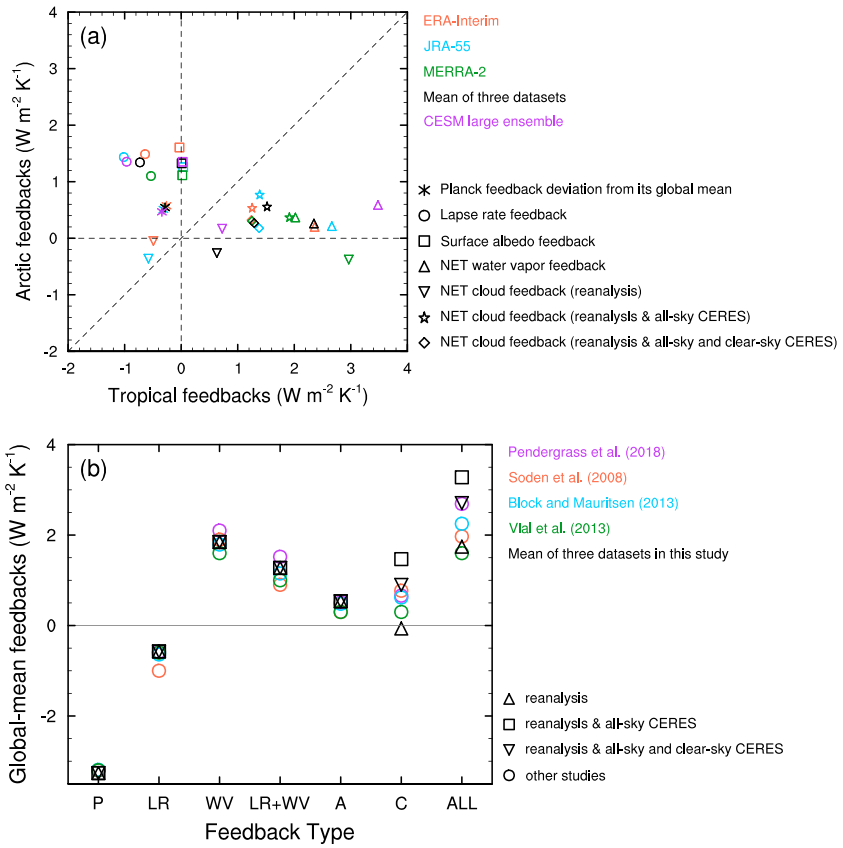


**Figure 3.** (a) Scatter plot of individual feedbacks ($W \cdot m^{-2} \cdot K^{-1}$) over the tropics and the Arctic. (b) Comparison of global-mean radiative feedbacks at the TOA ($W \cdot m^{-2} \cdot K^{-1}$). Detailed values are summarized in Table S10. The legends of colors and symbols for panel (a) and (b) are shown on the right-hand side of the corresponding panel. The reanalysis and CERES data sets used in both panels are for the period of March 2000 to September 2017.

and S5, the feedbacks estimated from the short-term climate variations are sensitive to the time periods considered because they are influenced by not only external forcing but also natural variability. Figure S9 shows the results derived from 38-year (1980–2017) reanalysis data sets. The relatively stable feature (Figure S9j) is that the relative importance of individual contributors to AA is the same as that in Figure 3a. However, except for the Planck and albedo feedbacks, there are larger differences at low latitudes than at high latitudes between the 38-year and 18-year results, especially for the cloud feedback (see Figure S10). Comparing to the 18-year results in Figures 3b and S8, except for the global mean Planck feedback, all feedbacks derived from 38-year reanalysis data sets have discernable differences, especially the WV and cloud feedbacks (see Figures S11 and S12). This also indicates that one should be cautious about using short-term climate feedbacks to constrain long-term climate sensitivity.

In summary, we investigate the local short-term feedbacks (including Planck, LR, surface albedo, WV, and cloud feedbacks) over the Arctic (60–90°N) from model/reanalysis data sets and observations using the combined Kernel-Gregory method. We diagnose the impact of data set choice on the feedback estimates for the shortwave, longwave, and net radiation. The inferred cloud feedback using the adjustment method mainly depends on the CRF (i.e., the all-sky minus the clear-sky TOA irradiance), while the choice of data sets for meteorological fields (albedo $\alpha$, temperature $T$, and moisture $q$) has a small impact. The results presented here show that all feedbacks are positive over the Arctic except for the uncertain cloud feedback. Both shortwave and longwave WV feedbacks are positive, leading to a significantly positive net WV feedback. The magnitudes of LR and albedo feedbacks are comparable. Relative to the tropics (30°S–30°N), the LR feedback is the largest contributor to AA, followed by the albedo feedback and Planck feedback deviation from its global mean. The WV feedback, however, has a negative contribution to AA relative to the tropics. Our analysis further confirms that the cloud feedback has the largest uncertainty, including its sign, which strongly

depends on the data set used for all-sky and clear-sky radiative fluxes at the TOA, the time period considered, and the method used to estimate the cloud feedback. Most of the uncertainty in cloud feedback is from its shortwave component. Our best estimates (mean of three data sets in Figure 3a) for Planck feedback deviation, LR, albedo, and net WV feedbacks over the Arctic are 0.54 ± 0.03, 1.34 ± 0.2, 1.33 ± 0.32, and 0.26 ± 0.1 $W \cdot m^{-2} \cdot K^{-1}$, respectively. Unfortunately, we are not confident to give an estimation for the net cloud feedback based on the current analysis, even its sign. Note that we have used the radiative kernels derived from CESM/CAM5 (Pendergrass et al., 2018) in the feedback calculations, which might introduce uncertainty to the results of each reanalysis data set. This warrants a future study to use radiative kernels derived from respective reanalysis background states to reexamine these feedbacks, especially cloud feedback in the Arctic.

**Acknowledgments**
We thank Nicole Feldl and Steve Warren for helpful discussions and/or comments on an early draft. This study was supported by the National Science Foundation of China (NSFC) (41605041), Jiangsu Provincial Science Fund (BK20160621), Fundamental Research Funds for the Central Universities (020714380020), Jiangsu Provincial 2011 program (Collaborative Innovation Center of Climate Change) and International Postdoctoral Exchange Fellowship (20160046), and by the U.S. Department of Energy (DOE) Office of Science, Biological and Environmental Research as part of the Regional and Global Climate Modeling program. The Pacific Northwest National Laboratory (PNNL) is operated for DOE by Battelle Memorial Institute under contract DE-AC05-76RLO1830. The model simulations were performed using PNNL Institutional Computing resources. The MERRA reanalysis was obtained from https://disc.sci.gsfc.nasa.gov/mdisc/, the JRA-55 reanalysis from http://jra.kishou.go.jp/JRA-55/index_en.html#download, and the ERA-Interim reanalysis from http://apps.ecmwf.int/datasets/data/interim-full-moda/levtype=pl/. The radiative kernel data are available at https://zenodo.org/record/997902. The CERES EBAF Ed4.0 data were downloaded at https://eosweb.larc.nasa.gov/project/ceres/ceres_table.

## References

Armour, K. C., Bitz, C. M., & Roe, G. H. (2013). Time-varying climate sensitivity from regional feedbacks. *Journal of Climate*, *26*(13), 4518–4534. https://doi.org/10.1175/JCLI-D-12-00544.1

Block, K., & Mauritsen, T. (2013). Forcing and feedback in the MPI-ESM-LR coupled model under abruptly quadrupled $CO_2$. *Journal of Advances in Modeling Earth Systems*, *5*(4), 676–691. https://doi.org/10.1002/jame.20041

Bony, S., Colman, R., Kattsov, V. M., Allan, R. P., Bretherton, C. S., Dufresne, J. L., et al. (2006). How well do we understand and evaluate climate change feedback processes? *Journal of Climate*, *19*(15), 3445–3482. https://doi.org/10.1175/JCLI3819.1

Bony, S., Stevens, B., Frierson, D. M. W., Jakob, C., Kageyama, M., Pincus, R., et al. (2015). Clouds, circulation and climate sensitivity. *Nature Geoscience*, *8*(4), 261–268. https://doi.org/10.1038/ngeo2398

Bosilovich, M. G., & Koster, R. D. (2015). MERRA-2: Initial evaluation of the climate. NASA Tech. Rep. Series on Global Modeling and Data Assimilation (NASA/TM–2015-104606/Vol. 43, pp. 145). Retrieved from https://gmao.gsfc.nasa.gov/pubs/docs/Bosilovich803.pdf

Cai, M., & Lu, J. (2007). Dynamical greenhouse-plus feedback and polar warming amplification. Part II: Meridional and vertical asymmetries of the global warming. *Climate Dynamics*, *29*(4), 375–391. https://doi.org/10.1007/s00382-007-0238-9

CERES Science Team (2017). Hampton, VA, USA: NASA Atmospheric Science Data Center (ASDC). https://doi.org/10.5067/Terra+Aqua/CERES/EBAF-TOA_L3B004.0 Accessed 11/11/2017

Charney, J. G., Arakawa, A., Baker, D. J., Bolin, B., & Dickinson, R. E. (1979). Carbon dioxide and climate: A scientific assessment. National Academy of Sciences Tech. Rep. (pp. 34). https://doi.org/10.17226/12181

Crook, J. A., Forster, P. M., & Stuber, N. (2011). Spatial patterns of modeled climate feedback and contributions to temperature response and polar amplification. *Journal of Climate*, *24*(14), 3575–3592. https://doi.org/10.1175/2011JCLI3863.1

Dalton, M. M., & Shell, K. M. (2013). Comparison of short-term and long-term radiative feedbacks and variability in twentieth-century global climate model simulations. *Journal of Climate*, *26*(24), 10,051–10,070. https://doi.org/10.1175/JCLI-D-12-00564.1

Dee, D. P., Uppala, S. M., Simmons, A. J., Berrisford, P., Poli, P., Kobayashi, S., et al. (2011). The ERA-Interim reanalysis: Configuration and performance of the data assimilation system. *Quarterly Journal of the Royal Meteorological Society*, *137*(656), 553–597. https://doi.org/10.1002/qj.828

Dessler, A. E. (2010). A determination of the cloud feedback from climate variations over the past decade. *Science*, *330*(6010), 1523–1527. https://doi.org/10.1126/science.1192546

Dessler, A. E. (2013). Observations of climate feedbacks over 2000–2010 and comparisons to climate models. *Journal of Climate*, *26*(1), 333–342. https://doi.org/10.1175/JCLI-D-11-00640.1

Eastman, R., & Warren, S. G. (2010a). Interannual variations of Arctic cloud types in relation to sea ice. *Journal of Climate*, *23*(15), 4216–4232. https://doi.org/10.1175/2010JCLI3492.1

Eastman, R., & Warren, S. G. (2010b). Arctic cloud changes from surface and satellite observations. *Journal of Climate*, *23*(15), 4233–4242. https://doi.org/10.1175/2010JCLI3544.1

Feldl, N., Bordoni, S., & Merlis, T. M. (2017). Coupled high-latitude climate feedbacks and their impact on atmospheric heat transport. *Journal of Climate*, *30*(1), 189–201. https://doi.org/10.1175/JCLI-D-16-0324.1

Feldl, N., & Roe, G. H. (2013). Four perspectives on climate feedbacks. *Geophysical Research Letters*, *40*, 4007–4011. https://doi.org/10.1002/grl.50711

Feldman, D. R., Collins, W. D., Pincus, R., Huang, X., & Chen, X. (2014). Far-infrared surface emissivity and climate. *Proceedings of the National Academy of Sciences of the United States of America*, *111*(46), 16,297–16,302. https://doi.org/10.1073/pnas.1413640111

Goosse, H., Kay, J. E., Armour, K. C., Bodas-Salcedo, A., Chepfer, H., Docquier, D., et al. (2018). Quantifying climate feedbacks in polar regions. *Nature Communications*, *9*(1), 1919. https://doi.org/10.1038/s41467-018-04173-0

Graversen, R. G., & Wang, M. (2009). Polar amplification in a coupled climate model with locked albedo. *Climate Dynamics*, *33*(5), 629–643. https://doi.org/10.1007/s00382-009-0535-6

Gregory, J. M., Ingram, W. J., Palmer, M. A., Jones, G. S., Stott, P. A., Thorpe, R. B., et al. (2004). A new method for diagnosing radiative forcing and climate sensitivity. *Geophysical Research Letters*, *31*, L03205. https://doi.org/10.1029/2003GL018747

Hall, A. (2004). The role of surface albedo feedback in climate. *Journal of Climate*, *17*(7), 1550–1568. https://doi.org/10.1175/1520-0442(2004)017<1550:TROSAF>2.0.CO;2

Hansen, J., Lacis, A., Rind, D., Russell, G., Stone, P., & Fung, I. (1984). Climate sensitivity: Analysis of feedback mechanisms. In *Climate Processes and Climate Sensitivity*, *Geophysical Monograph Series* (Vol. 29, pp. 130–163). Washington, DC: American Geophysical Union. https://doi.org/10.1029/GM029p0130

Held, I. M., & Soden, B. J. (2000). Water vapor feedback and global warming. *Annual Review of Energy and the Environment*, *25*(1), 441–475. https://doi.org/10.1146/annurev.energy.25.1.441

Huang, J., Zhang, X., Zhang, Q., Lin, Y., Hao, M., Luo, Y., et al. (2017). Recently amplified arctic warming has contributed to a continual global warming trend. *Nature Climate Change*, *7*(12), 875–879. https://doi.org/10.1038/s41558-017-0009-5

Huang, X., Chen, X., Flanner, M., Yang, P., Feldman, D., & Kuo, C. (2018). Improved representation of surface spectral emissivity in a global climate model and its impact on simulated climate. *Journal of Climate*, *31*, 3711–3727. https://doi.org/10.1175/JCLI-D-17-0125.1

Hwang, J., Choi, Y. S., Kim, W. M., Su, H., & Jiang, J. H. (2017). Observational estimation of radiative feedback to surface air temperature over northern high latitudes. *Climate Dynamics*, *50*(1–2), 615–628. https://doi.org/10.1007/s00382-017-3629-6

Intergovernmental Panel on Climate Change (IPCC) (2013). Climate change 2013: The physical science basis. In T. F. Stocker, et al. (Eds.), *Contribution of Working Group I to the Fifth Assessment Report of the Intergovernmental Panel on Climatse Change* (1535 pp.). Cambridge, UK and New York: Cambridge University Press.

Kobayashi, S., Ota, Y., Harada, Y., Ebita, A., Moriya, M., Onoda, H., et al. (2015). The JRA-55 reanalysis: General specifications and basic characteristics. *Journal of the Meteorological Society of Japan. Ser. II*, *93*(1), 5–48. https://doi.org/10.2151/jmsj.2015-001

Koumoutsaris, S. (2013). What can we learn about climate feedbacks from short-term climate variations? *Tellus A*, *65*(1), 18887. https://doi.org/10.3402/tellusa.v65i0.18887

Liu, X., Ma, P. L., Wang, H., Tilmes, S., Singh, B., Easter, R. C., et al. (2016). Description and evaluation of a new 4-mode version of Modal Aerosol Module (MAM4) within version 5.3 of the Community Atmosphere Model. *Geoscientific Model Development*, *9*(2), 505–522. https://doi.org/10.5194/gmd-9-505-2016

Loeb, N. G., Doelling, D. R., Wang, H., Su, W., Nguyen, C., Corbett, J. G., et al. (2018). Clouds and the Earth's Radiant Energy System (CERES) Energy Balanced and Filled (EBAF) Top-of-Atmosphere (TOA) Edition-4.0 Data Product. *Journal of Climate*, *31*, 895–918. https://doi.org/10.1175/JCLI-D-17-0208.1

Loeb, N. G., Wielicki, B. A., Doelling, D. R., Smith, G. L., Keyes, D. F., Kato, S., et al. (2009). Toward optimal closure of the Earth's top-of-atmosphere radiation budget. *Journal of Climate*, *22*(3), 748–766. https://doi.org/10.1175/2008JCLI2637.1

Ma, P.-L., Rasch, P. J., Wang, H., Zhang, K., Easter, R. C., Tilmes, S., et al. (2013). The role of circulation features on black carbon transport into the Arctic in the Community Atmosphere Model version 5 (CAM5). *Journal of Geophysical Research: Atmospheres*, *118*, 4657–4669. https://doi.org/10.1002/jgrd.50411

Manabe, S., & Wetherald, R. T. (1975). The effects of doubling the $CO_2$ concentration on the climate of a general circulation model. *Journal of the Atmospheric Sciences*, *32*(1), 3–15. https://doi.org/10.1175/1520-0469(1975)032<0003:TEODTC>2.0.CO;2

Neale, R. B., J. H. Richter, A. J. Conley, S. Park, P. H. Lauritzen, A. Gettelman, et al. (2010). Description of the NCAR Community Atmosphere Model (CAM5), (Tech. Rep. NCAR/TN-486+STR, pp. 268). Boulder, CO: National Center for Atmospheric Research.

Pendergrass, A. G., Conley, A., & Vitt, F. M. (2018). Surface and top-of-atmosphere radiative feedback kernels for CESM-CAM5. *Earth System Science Data*, *10*(1), 317–324. https://doi.org/10.5194/essd-10-317-2018

Pithan, F., & Mauritsen, T. (2014). Arctic amplification dominated by temperature feedbacks in contemporary climate models. *Nature Geoscience*, *7*(3), 181–184. https://doi.org/10.1038/ngeo2071

Po-Chedley, S., Armour, K. C., Bitz, C. M., Zelinka, M. D., Santer, B. D., & Fu, Q. (2018). Sources of intermodel spread in the lapse rate and water vapor feedbacks. *Journal of Climate*, *31*(8), 3187–3206. https://doi.org/10.1175/JCLI-D-17-0674.1

Rienecker, M. M., Suarez, M. J., Gelaro, R., Todling, R., Bacmeister, J., Liu, E., et al. (2011). MERRA: NASA's Modern-Era Retrospective Analysis for Research and Applications. *Journal of Climate*, *24*(14), 3624–3648. https://doi.org/10.1175/JCLI-D-11-00015.1

Roe, G. H., Feldl, N., Armour, K. C., Hwang, Y.-T., & Frierson, D. M. W. (2015). The remote impacts of climate feedbacks on regional climate predictability. *Nature Geoscience*, *8*(2), 135–139. https://doi.org/10.1038/ngeo2346

Rose, B. E. J., Armour, K. C., Battisti, D. S., Feldl, N., & Koll, D. D. B. (2014). The dependence of transient climate sensitivity and radiative feedbacks on the spatial pattern of ocean heat uptake. *Geophysical Research Letters*, *41*, 1071–1078. https://doi.org/10.1002/2013GL058955

Screen, J. A., & Simmonds, I. (2010). The central role of diminishing sea ice in recent Arctic temperature amplification. *Nature*, *464*(7293), 1334–1337. https://doi.org/10.1038/nature09051

Shell, K. M., Kiehl, J. T., & Shields, C. A. (2008). Using the radiative kernel technique to calculate climate feedbacks in NCAR'S community atmospheric model. *Journal of Climate*, *21*(10), 2269–2282. https://doi.org/10.1175/2007JCLI2044.1

Soden, B. J., & Held, I. M. (2006). An assessment of climate feedbacks in coupled ocean-atmosphere models. *Journal of Climate*, *19*(14), 3354–3360. https://doi.org/10.1175/JCLI3799.1

Soden, B. J., Held, I. M., Colman, R., Shell, K. M., Kiehl, J. T., & Shields, C. A. (2008). Quantifying climate feedbacks using radiative kernels. *Journal of Climate*, *21*(14), 3504–3520. https://doi.org/10.1175/2007JCLI2110.1

Taylor, K. E., Stouffer, R. J., & Meehl, G. A. (2012). An overview of CMIP5 and the experiment design. *Bulletin of the American Meteorological Society*, *93*(4), 485–498. https://doi.org/10.1175/BAMS-D-11-00094.1

Taylor, P. C., Cai, M., Hu, A., Meehl, J., Washington, W., & Zhang, G. J. (2013). A decomposition of feedback contributions to polar warming amplification. *Journal of Climate*, *26*(18), 7023–7043. https://doi.org/10.1175/JCLI-D-12-00696.1

Vavrus, S. (2004). The impact of cloud feedbacks on Arctic climate under greenhouse forcing. *Journal of Climate*, *17*(3), 603–615. https://doi.org/10.1175/1520-0442(2004)017<0603:TIOCFO>2.0.CO;2

Vial, J., Dufresne, J.-L., & Bony, S. (2013). On the interpretation of inter-model spread in CMIP5 climate sensitivity estimates. *Climate Dynamics*, *41*(11-12), 3339–3362. https://doi.org/10.1007/s00382-013-1725-9

Wang, H., Easter, R. C., Rasch, P. J., Wang, M., Liu, X., Ghan, S. J., et al. (2013). Sensitivity of remote aerosol distributions to representation of cloud-aerosol interactions in a global climate model. *Geoscientific Model Development*, *6*(3), 765–782. https://doi.org/10.5194/gmd-6-765-2013

Wang, H., Rasch, P. J., Easter, R. C., Singh, B., Zhang, R., Ma, P. L., et al. (2014). Using an explicit emission tagging method in global modeling of source-receptor relationships for black carbon in the Arctic: Variations, sources, and transport pathways. *Journal of Geophysical Research: Atmospheres*, *119*, 12,888–12,909. https://doi.org/10.1002/2014JD022297

Winton, M. (2006). Amplified Arctic climate change: What does surface albedo feedback have to do with it? *Geophysical Research Letters*, *33*, L03701. https://doi.org/10.1029/2005GL025244

Yang, Y., Wang, H., Smith, S. J., Ma, P. L., & Rasch, P. J. (2017). Source attribution of black carbon and its direct radiative forcing in China. *Atmospheric Chemistry and Physics*, *17*(6), 4319–4336. https://doi.org/10.5194/acp-17-4319-2017

Zelinka, M. D., & Hartmann, D. L. (2012). Climate feedbacks and their implications for poleward energy flux changes in a warming climate. *Journal of Climate*, *25*(2), 608–624. https://doi.org/10.1175/JCLI-D-11-00096.1

Zelinka, M. D., Klein, S. A., Taylor, K. E., Andrews, T., Webb, M. J., Gregory, J. M., & Forster, P. M. (2013). Contributions of different cloud types to feedbacks and rapid adjustments in CMIP5. *Journal of Climate*, *26*(14), 5007–5027. https://doi.org/10.1175/JCLI-D-12-00555.1

Zhou, C., Zelinka, M. D., Dessler, A. E., & Yang, P. (2013). An analysis of the short-term cloud feedback using MODIS data. *Journal of Climate*, *26*(13), 4803–4815. https://doi.org/10.1175/JCLI-D-12-00547.1